Synthetic and Mechanistic Studies into the Reductive Functionalization of Nitro Compounds Catalyzed by an Iron(salen) Complex

Emily Pocock,[a] Martin Diefenbach,[†b] Thomas M. Hood,[†a] Michael Nunn,[c] Emma Richards,*[d] Vera Krewald*[b] and Ruth L. Webster*[e]

a Department of Chemistry, University of Bath, Claverton Down, Bath, United Kingdom, BA2 7AY.

b Department of Chemistry, TU Darmstadt, 64287 Darmstadt, Germany.

c Early Chemical Development, Pharmaceutical Sciences, Biopharmaceuticals R&D, AstraZeneca, Macclesfield, United Kingdom, SK10 2NA.

d School of Chemistry, Cardiff University, Main Building, Park Place, Cardiff, United Kingdom, CF10 3AT.

e Yusuf Hamied Department of Chemistry, University of Cambridge, Lensfield Road, Cambridge, United Kingdom, CB2 1EW.

Supporting Information Placeholder

ABSTRACT: We report on the use of a simple, bench stable [Fe(salen)$_2$]-μ-oxo pre-catalyst in the reduction of nitro compounds. The reaction proceeds at room temperature across a range of substrates, including nitro aromatics and aliphatics. By changing the reducing agent from pinacol borane (HBpin) to phenyl silane (H_3SiPh) we can chemoselectively reduce nitro compounds while retaining carbonyl functionality. Our mechanistic studies, which include kinetics, EPR, mass spectrometry and quantum chemistry, indicate the presence of a nitroso intermediate and the generation of an on-cycle iron-hydride as a key catalytic intermediate. Based on this mechanistic insight we were able to extend the chemistry to hydroamination and identified a simple substrate feature (alkene LUMO energy) that could be used to predict which alkenes would result in productive catalysis.

INTRODUCTION

Traditionally, the reduction of a nitro moiety to its corresponding primary amine is carried out under harsh conditions (for example, a metal with concentrated acid at high temperature),[1] and although an iron(0)/acetic acid route was reported as early as 1854,[2, 3] milder methods have since been established.[4] Pertinent to this homogeneous catalysis work is that simple iron salts have been shown to catalyze the reduction of nitroaromatics,[5, 6] for example Nagashima's use of $Fe_3(CO)_{12}$ (Scheme 1a),[7] Beller's use of $FeBr_2$ (scheme 1b)[8] and $Fe(acac)_3$ has been employed by Lemaire and co-workers,[9, 10] but these reactions often requiring forcing conditions. A range of ligated iron complexes have also been employed with silanes,[11-15] or alternative hydride/hydrogen donors[16-25] as reducing agents. More recently still, Mo reported a well-defined molecular iron catalyst capable of reducing nitro compounds under mild conditions,[26] in this case it is believed that the cooperative nature of the Fe–Si bond in the catalyst is necessary to facilitate these reductions (Scheme 1c).

Baran and co-workers' seminal study on *in situ* hydroamination (HA) of olefins using nitro aromatics as the nitrogen source (Scheme 1d)[27] has led to several analogous iron-catalyzed studies featuring both intra-[28-35] and intermolecular[11, 28] HA. Baran's work exemplifies the capacity of this transformation through the report of substituent-diverse synthesis of secondary amines from a range of nitro aromatics. There are some limitations in the substrate scope: free thiophenol and phenol-nitros are not tolerated and the olefin coupling partner must contain aliphatic substituents. On the other hand, Wang and co-workers have developed an iron(Cp*) system that operates across a range of styrenes.[28] However, it is important to stress how challenging this transformation is based on the postulated mechanism: iron-catalyzed partial reduction of the nitro group to a nitroso is necessary, which then must be trapped by an alkyl radical formed from a hydrogen atom transfer (HAT) event that is mediated by the same iron species. Therefore, there is the need to balance high activity while avoiding over-reduction (i.e. reduction of the nitro to an amine) and runaway radical reactions (i.e. alkene polymerization). Thus, iron-mediated intermolecular HA from nitro compounds remains a challenge.

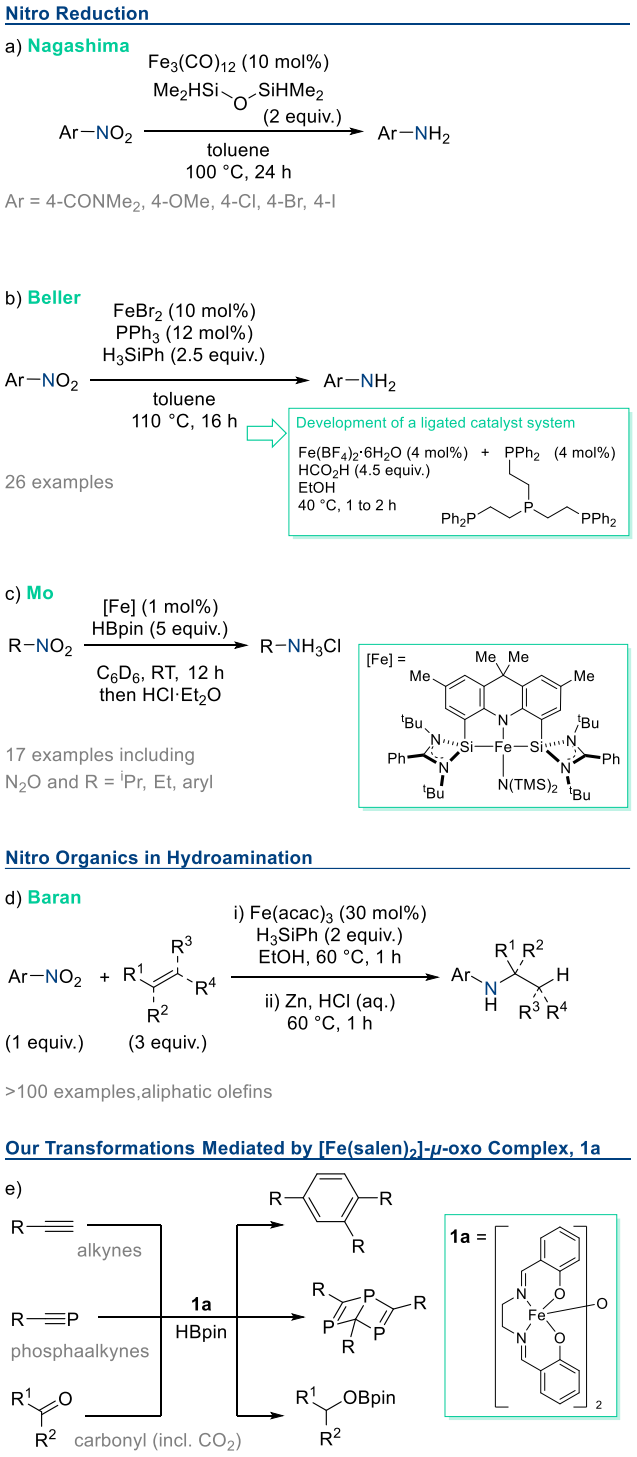

Scheme 1. Previous work on iron-catalyzed nitro reduction includes a) early work from Nagashima using an iron carbonyl compound, followed by b) research from Beller using $FeBr_2$, which then led to a phosphine-ligated system, and c) more recently Mo has used an iron-silylene pre-catalyst. Intercepting the nitro reduction process allowed d) seminal studies from Baran into iron catalyzed hydroamination; e) our previous studies using precatalyst **1a** and HBpin has included cyclotrimerization and carbonyl reduction.

Previous work in our group has focused on the use of iron(salen) complexes and these have proven to be highly active in hydrophosphination,[36, 37] hydroboration,[38] organo-alkyne[39, 40] and phosphaalkyne[26] cyclotrimerization (Scheme 1e). These complexes benefit from being air stable with a scalable synthesis. They are also highly tunable (via the ligand)[41-45] and thus more soluble, and potentially more active and selective, than iron salts or *in situ* formed complexes. Our previous studies have indicated that we may be able to access a particularly 'hot' (i.e. reactive) iron(salen)-hydride species[40] and we postulated that we should be able to sequester this for fast and facile reduction chemistry. The short-lived nature of the iron hydride means that an appropriate target substrate is needed. To this end we have found that nitro compounds are an ideal substrate for reduction using Fe(salen)-μ-oxo (**1a**) as the pre-catalyst and HBpin as the reductant. We herein present the results of our synthetic scope of nitro reduction, associated mechanistic studies and the extension to HA which is driven by predictive density functional theory (DFT) studies (Scheme 2).

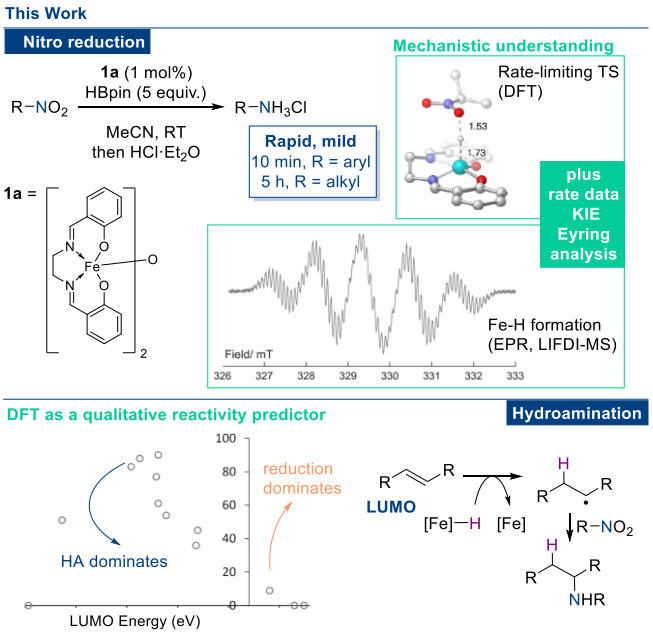

Scheme 2. The research presented herein shows the development of a mild nitro reduction protocol using a simple, air stable pre-catalyst. Our mechanistic studies indicate the presence of a nitroso intermediate, which is then exploited in hydroamination.

RESULTS AND DISCUSSION

2.1 Nitro Reduction Scope

Following a short optimization study (see the Supporting Information), treatment of a range of nitro compounds with 1 mol% pre-catalyst **1a** and 5 equivalents of HBpin in acetonitrile results in facile reduction across a range of substrates in only 10 minutes at room temperature. No reaction is observed in the absence of **1a**. Reduction does take place when H_3SiPh (2 equivalents) is employed, but the reaction requires heating to 50 °C for 16 h (see the Supporting Information). Purification by column chromatography results in considerable loss of the desired primary amine. Instead, formation of the ammonium salt by treatment with HCl in Et_2O is an operationally simple method of isolation (Figure 1). Generally, good to excellent spectroscopic yields are achieved for nitroaromatics bearing both electron-donating and withdrawing substituents, with

good functional group tolerance (**3a** to **3k**). Most notably, substrates bearing 'free' thiophenol and phenol moieties (generating products **3e** and **3j** respectively) are extremely well tolerated under our conditions. Such protic substrates are typically not well tolerated under nitro reduction conditions (or are, at least, unreported). In our case, the addition of an additional equivalent of HBpin (totaling 6 equivalents) facilitates an *in situ* dehydrocoupling[46] of the phenol moiety (see Supporting Information for NMR analysis of **3j**, which contains N-Bpin and O-Bpin protected functionality), thus preventing any potential catalytic poisoning. **3h** is derived from the aldehyde and requires an extra equivalent of HBpin in order to facilitate clean reduction of the aldehyde and the nitro group (*vide infra*). For comparison, Beller's work using 4.5 equiv. formic acid at 40 °C for 1 hour operates well across a range of halogenated substrates along with vinyl-, methoxy- and methylsulfane-substituted nitro aromatics,[23] while Mo has demonstrated nitro aromatics can be cleanly reduced using HBpin without adversely affecting heteroaromatic and cyano functionality.[26] Our substrate scope is not exhaustive, but we can state that pyridyl-, pyrimidinedione-, and carboxylic acid-containing substrates fail under our standard reaction conditions.

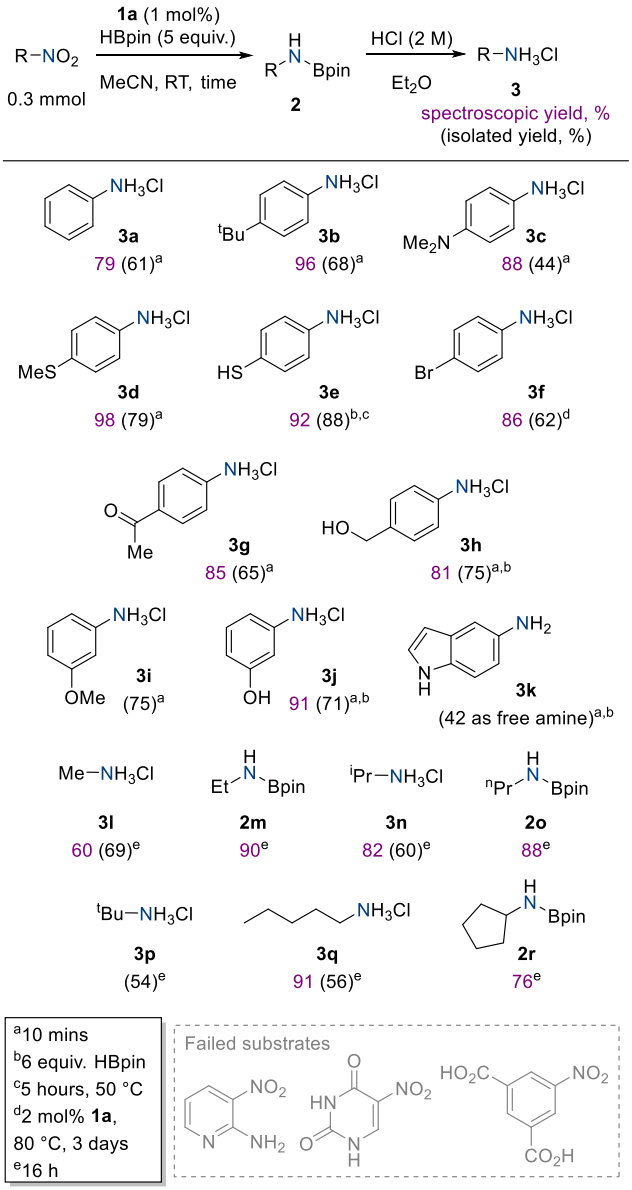

Figure 1. Substrate scope for the reduction of nitro compounds using HBpin and pre-catalyst **1a**.

The iron-catalyzed reduction of nitro aliphatics is surprisingly sparce in the literature. Mo and co-workers demonstrated the competent reduction of nitrous oxide as well as nitroethane and 2-nitropropane,[26] but other studies tend to omit these more challenging substrates. Gratifyingly, our conditions are readily applied to a small number of aliphatic nitro compounds (Figure 1, generating salt products **3l**, **3n**, **3p**, **3q** and Bpin adducts to **2m**, **2o** and **2r**), including nitromethane (to form **3l**). The reaction proceeds smoothly at room temperature, but the reactions have been left for 16 h to ensure they go to completion. This methodology serves as an attractive tool for the *in situ* generation of anhydrous methylamine.

Due to the high levels of catalytic activity we observe, 4-nitrobenzaldehyde undergoes reduction at both the nitro and carbonyl groups (Figure 1 and Scheme 3a). This reduction proceeds via hydroboration of the aldehyde, which we have previously demonstrated occurs readily in the presence of pre-catalyst **1a** under similar reaction conditions.[38] We hypothesized that changing the highly active reductant, HBpin, for a

less active one, e.g. H_3SiPh, should allow us to chemoselectively reduce the nitro group and leave the aldehyde intact. This is the case: H_3SiPh allows the smooth reduction of the nitro-moiety without considerable reduction of the aldehyde unit (Scheme 3b). The reduced yield for this reaction is due to the formation of an unknown polymeric precipitate but boasts greater overall chemoselectivity.

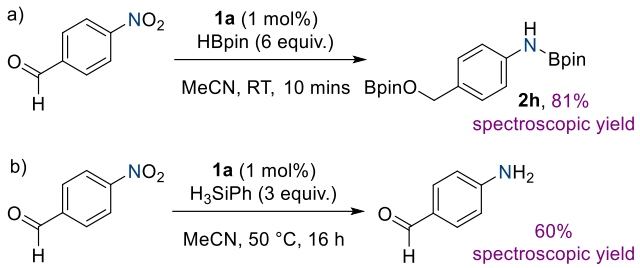

Scheme 3. A change in reducing agent from HBpin (a) to H_3SiPh (b) allows for chemoselective reduction.

2.2 Mechanistic Studies

To begin our mechanistic investigation, we identified a range of possible N–O intermediates and exposed them to our catalytic conditions. A nitrosoarene, an *N*-alkoxyaniline and an oxime (**4a**, **5a** and **7a**, respectively, Figure 2) were subjected to the reduction conditions to probe their plausibility as intermediates. Nitrosobenzene (**4a**, Figure 2a) forms **2a** in 87% spectroscopic yield under standard reaction conditions. **4a** can be reduced to **2a** using HBpin in the absence of **1a**, but requires 18 h at 80 °C to do so.

N-phenylhydroxylamine (**5a**) is reduced to **2a** in 72% spectroscopic yield over an extended time period (Figure 2b). Interestingly, *in situ* NMR monitoring shows an appreciable buildup of azoxybenzene (**6a**) and azobenzene (**6a'**) after 20 minutes at RT. This clearly indicates a switch in mechanism, one where these N–N coupled products are intermediates. These intermediates are not observed during *in situ* NMR monitoring of the reduction of nitrobenzene, and coupled with the extended timescale of this process indicates hydroxylamines, although reducible, are not intermediates in our nitro reduction catalysis. This trend is also observed when $HSi(OEt)_3$ is used as a reductant (see the Supporting Information).

Monitoring the reaction by NMR spectroscopy using a nitrosobenzene (**4a**), rather than a nitrobenzene, is challenging due to the fast nature of the reaction. To gain insight and useful reaction profiles, $HSi(OEt)_3$ was employed as the reductant. Based on the reaction profiles obtained (Figure 2c) it can be further confirmed that nitrosobenzene is likely to be a short-lived intermediate and does not build up in the reaction, because using nitrosobenzene as a drop-in replacement for nitrobenzene results in its zeroth order decay and rapid formation of azoxybenzene (approximately 20% after 95 minutes), which then depletes over the remainder of the reaction period as aniline continues to form. In contrast, under identical rection conditions over the same time period using nitrobenzene (Figure 2d), we see clean conversion to aniline with no intermediate **6a** being observed. There is a slower induction-type phase to catalysis that is not observed when starting from **4a**. This is likely linked to the fact that the silane is not as effect at converting the pre-catalyst into active catalyst. Unfortunately, the difference in reactivity of PhNO compared to $PhNO_2$ has also meant we cannot deconvolute the proposed interlinked catalytic cycles (*vide infra*).

The reduction of nitro compounds is clean and only $(pinB)_2O$ (δ_{11B} 21 ppm) and dihydrogen (δ_{1H} 4.57 ppm) are observed. During these kinetic studies nitrosobenzene is also not detected, further indicating that it is a short-lived intermediate *en route* to product formation. However, the timescale of the reduction of **4a** to aniline via **6a** using $HSi(OEt)_3$ (Figure 2c) is in-line with silane-mediated reduction of nitrobenzene to aniline (Figure 2d) and therefore we feel a nitroso intermediate is likely.

In contrast, oxime **7a** quantitatively dehydrocouples with HBpin to generate **7a-Bpin** and no further reduction can be facilitated (Figure 2e). Oximes can be ruled out as intermediates.

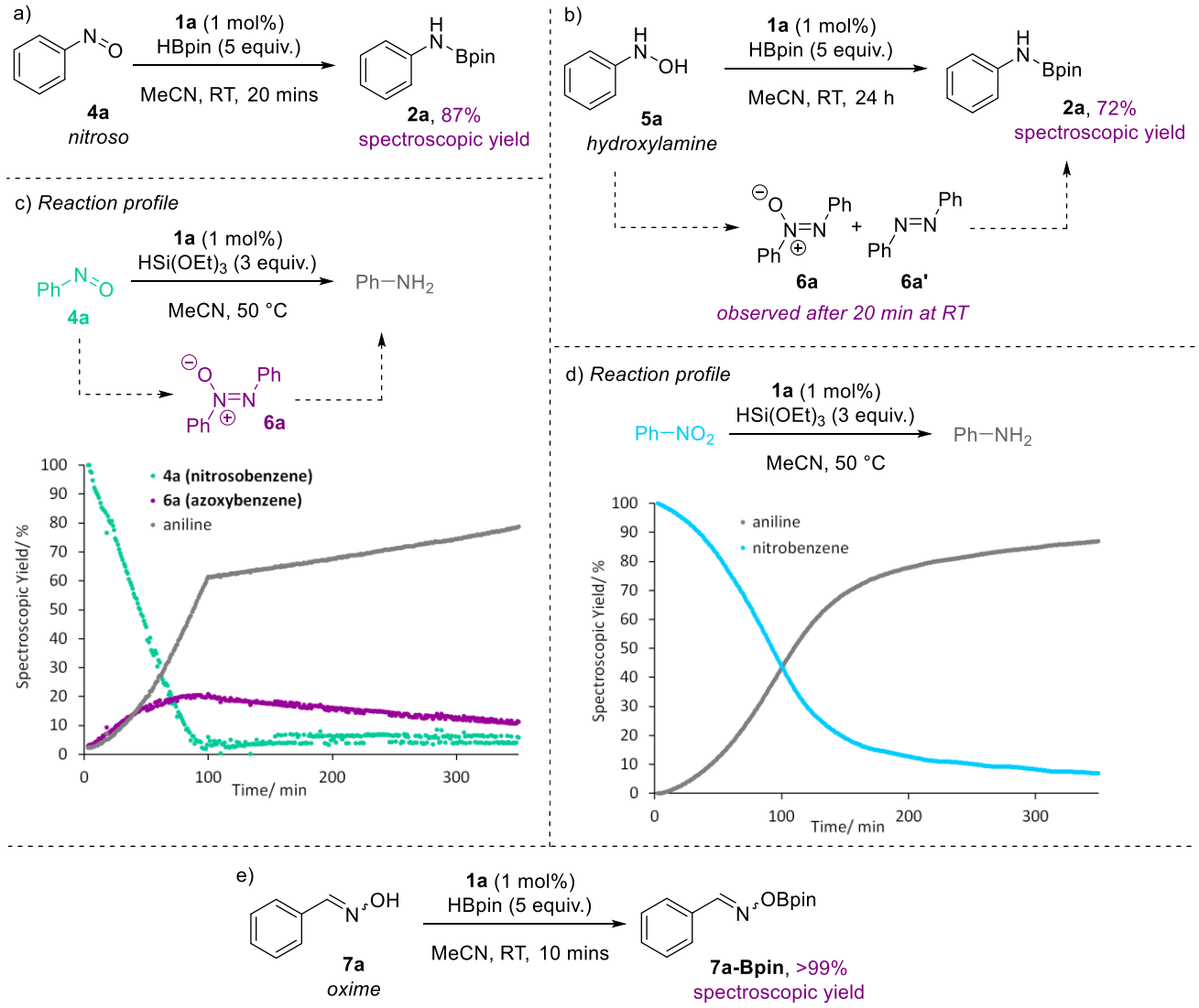

Figure 2. Investigation into likely intermediates formed during nitro reduction catalyzed by **1a**. a) Reaction of a nitroso compounds under catalysis conditions; b) a hydroxylamine proceeds via intermediates **6a** and **6a'** and over a longer time period than standard catalysis; c) reaction profile showing the conversion of a nitroso in the presence of a silane, via **6a** (data collected every 60 sec); d) nitrobenzene converts cleanly to aniline in the presence of silane (data collected every 60 sec); e) a hydoxylamine is an unlikely intermediate as dehydrocoupling is observed.

The related pre-catalyst [Fe(II)salen] (**1b**, high spin, S = 2), which we could envision forms from reduction of **1a**, is active in catalysis. However, based on our previous work, reaction of **1a** to form [Fe(III)(H)salen] (**1c**) and elimination of H_2 from [Fe(H)salen]$_2$ to form **1b**[40] is slower than the reduction of a nitro compound, so this process is unlikely. EPR studies also show that **1a** and **1b** behave very differently indicating that **1b** is not involved in the catalytic cycle.[47, 48] It is important to note that the spectrum of **1a** (120 K, X-band) is characteristic of Fe(III) (see the Supporting Information), whilst **1b** (S = 2) is not observed by EPR (140 K, X-band) and is thus EPR-silent. Reaction of **1a**, **4c** and HBpin gives an EPR-silent spectrum at 298 K (*i.e.* no organo-radicals are detected) whereas reaction of **1b** with **4c** gives a nitroso radical cation, observed at 298 K (Figure 3a). Oxidation of **1b** to Fe(III) is also observed, as evidenced by the characteristic signal at 140 K. Unlike the results with **1a** in the presence of reducing agent, there is clear evidence of an organic radical species in the 298 K spectrum.

That organo radicals are not involved in our nitro reduction catalysis is further supported through a series of synthetic trapping experiments. Addition of 1 equivalent TEMPO to 2-nitropropane, HBpin (5 equiv.) and **1a** (1 mol%) gives **2n** in 60% spectroscopic yield, with the reaction going to 71% spectroscopic yield after another equivalent of HBpin is added (in this case we believe TEMPO is interfering with reactivity by reacting with the B–H bond). Adding 1 equivalent of chloromethylcyclopropane to 2-nitropropane, HBpin (5 equiv.) and 1a (1 mol%) gives 76% spectroscopic yield of **2n**, compared to 80% observed in the absence of a trapping agent.[49]

When nitrobenzene is employed in an *in situ* EPR study with **1a** and HBpin the reaction is EPR silent at 298 K (again, no organo-radicals are observed). In contrast, the production of a nitroxide radical is observed when complex **1b** is reacted with nitromethane in the absence of HBpin, evidenced by a 1:1:1 triplet signal originating from the ^{14}N nucleus (Figure 3b).

The *in situ* monitoring of the reaction of **1a** with HBpin by LIFDI-MS (Liquid Injection Field Desorption Ionization Mass Spectrometry) indicates the presence of a short-lived iron(III) hydride (**1c**; [Fe(III)(H)salen]). No further intermediates can be identified unambiguously by LIFDI-MS and there is no parent ion associated with **1b** (see the Supporting Information), adding further weight to the assertion that this species is not present in catalysis. ESI LCMS (Electrospray Ionisation Liquid Chromatography Mass Spectrometry) has also been used to identify the analogous deuteride [Fe(III)(D)salen] (see the Supporting Information).

The likely presence of **1c** is further supported through EPR studies, where reaction of **1a** and HBpin or H_3SiPh in the presence of a spin trapping agent (DMPO, 5,5-dimethyl-pyrroline *N*-oxide or PBN, *N*-tertiary-butyl nitrone) results in hydride trapping (see the Supporting Information).

Electronic structure calculations predict **1b** as a high spin species using Hartree–Fock and Kohn–Sham-DFT based coupled cluster theory in the DLPNO-CCSD(T) variant in agreement with our previous work (see the SI for details).[40] For the hydride species **1c**, the situation is less clear cut: HF-DLPNO-CCSD(T) predicts a high spin ground state with a energetically higher-lying low spin configuration (ΔG = 5.2 kcal/mol, Table S9), whereas KS-DLPNO-CCSD(T) predicts the reverse situation with the low spin state stabilized over the high spin state (ΔG = 3.6 kcal/mol). The implications for the catalytic cycle are discussed below and in the SI.

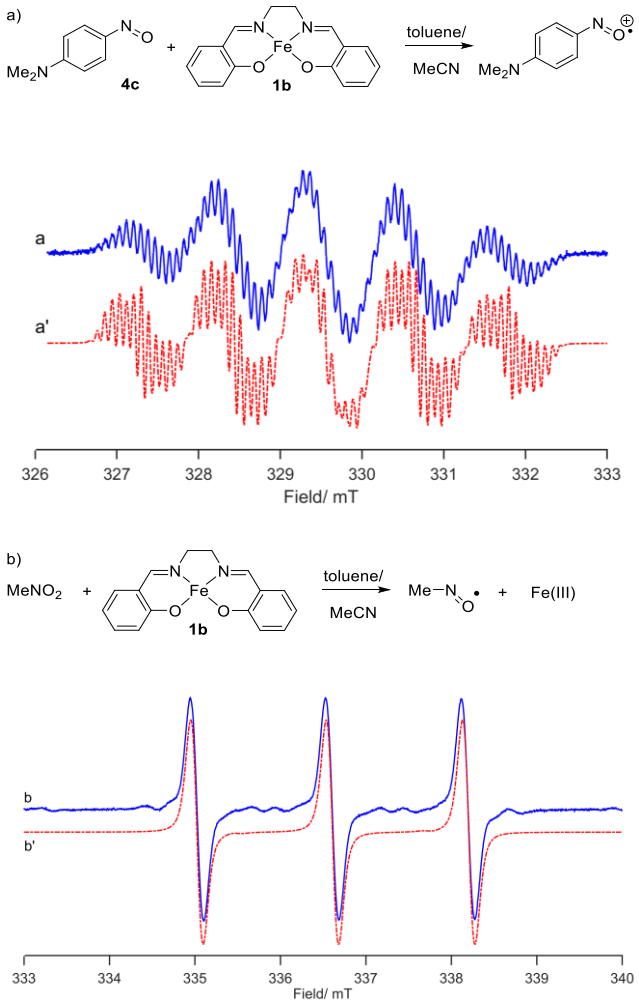

Figure 3. a) **1b** and **4c** generate a nitroso radical cation, whereas only an EPR-silent spectrum is observed with **1a** is reacted with HBpin and **4c**; b) nitromethane and **1b** generate a nitroxide radical. Corresponding simulations are presented in a' and b' (see the Supporting Information for details).

To obtain kinetics data we employed iPrNO2 and HBpin to allow adequate data collection. However, these reactions suffered from high levels of paramagnetism in the first 10 to 20 minutes, meaning initial rate data could not be collected. Therefore, by using $HSi(OEt)_3$ as the reducing agent and measuring the initial rates of reduction of $PhNO_2$, the reaction is found to be approximately ½-order in pre-catalyst **1a**. This is consistent with the formation of a monomeric active species *e.g.* mononuclear iron-hydride, **1c**. Its sensitivity is such that we have not been able to isolate **1c** and employ this in catalysis. Monitoring the overall reaction using HBpin as the reducing agent, where almost instantaneous pre-catalyst activation takes place, the reaction appears to be 1st order in on-cycle iron, indicating the mononuclear species does not undergo dimerization during catalysis. The reaction is first order in 2-nitropropane. At catalytically relevant regimes (4.5, 5.0 and 5.5 equivalents HBpin), the reaction is zero order in HBpin, consistent with the reductant not being involved in the rate-limiting step. At higher loadings of HBpin (6.75, 7.5 and 10 equiv.) the data does not fit zero or 1st order VTNA[50] or integrated rate law plots. At this point we assume that a change in mechanism and/or rate limiting step is taking place.

When DBpin is used, a KIE of 1.13 ± 0.09 was measured. This indicates that HBpin is unlikely to be involved in the rate-limiting step. However, although large primary KIEs have been reported for B–H bond cleavage,[51] small isotope effects have also been observed in hydride transfer reactions.[51–53] All deuterium incorporation is limited to the amine protons.

Eyring analysis using k_{obs} data from the reduction of 2-nitropropane with 1 mol% **1a**, 5 equivalents HBpin over a range of temperatures gives $\Delta G^{\ddagger}$ = 22.4 ± 4.0 kcal mol^{-1}, $\Delta H^{\ddagger}$ = 18.3 ± 1.1 kcal mol^{-1} and $\Delta S^{\ddagger}$ = –14.0 ± 3.8 cal mol^{-1} K^{-1}. These data are consistent with an early transition state, which is likely to be associative in nature, and a moderate barrier for the rate-limiting transition state, which is consistent with the facile (exergonic) nature of these nitro reduction reactions.

Based on the experimental data collected, we postulate that the reaction proceeds via the following interlinked catalytic cycles (Figure 4). Pre-catalyst **1a** is activated by HBpin (or silane), resulting in the iron(III) hydride species **1c**. This is evidenced by EPR showing that the reducing agents both generate a hydride that can be spin trapped, and LIFDI-MS data which shows the presence of **1c** in a catalytic run. **1c** interacts with the nitro reactant, then hydride transfer takes place. This is the rate-limiting step and has an experimentally determined barrier of 22.4 ± 4.0 kcal mol^{-1}. An iron(III) hydroxide is then generated, along with release of the nitroso intermediate, **4**. The hydroxide intermediate reacts with 2 equivalents HBpin to ultimately regenerate **1c**, releasing H_2 and pinBOBpin en route (the latter are observed by ^{1}H and ^{11}B NMR spectroscopy). **1c** further reacts with the nitroso intermediate, which is a very short-lived species. Another insertion reaction takes place, along with H_2 and pinBOBpin release, and the generation of an iron(III) amido species. The final step in the interlinked cycles is reaction of the iron(III) amido with HBpin to release product (**2**) and regenerate **1c**. The complexities of this

interlinked catalytic system has likely imparted a level of complexity to the kinetic data that we cannot deconvolute using standard VTNA or integrated rate law methods.

For the *in silico* evaluation of the interlinked catalytic cycles, the small energy gap between the high-spin and low-spin configurations of **1c** raises the question whether multistate reactivity will play a role. We find that all iron-containing intermediates have high-spin ground states at the density functional theory level PBE0-D3/def2-TZVP//PBE-D3/def2-SVP, which was benchmarked against HF-DLPNO-CCSD(T) calculations for **1b**, **1c** and the hydroxy intermediate (see the SI, Table S9). The catalytic sequence is therefore computed on the high-spin surface throughout.

The interlinked catalytic cycles were evaluated computationally for the substrates 2-nitropropane and nitrobenzene; we discuss here explicitly the 2-nitropropane case. The rate-limiting transition state for hydride transfer from **1c** to 2-nitropropane obtained by DFT is fully consistent with the experimentally derived Eyring analysis. The barrier for this step is calculated at $\Delta G^{\ddagger}$ = 19.8 kcal mol^{-1}, equivalent to $t_{1/2} \approx 27$ s. This is close to the computed BDFE for the iron-hydride bond of 18.7 kcal mol^{-1} at the same level of theory. As the next intermediate in the catalytic cycle, a nitroso–iron hydroxide complex is formed ($\Delta_r G$ = –9.5 kcal mol^{-1}). The barrier for liberating the short-lived nitroso intermediate is minute, $\Delta G^{\ddagger}$ = 2.5 kcal mol^{-1} (see SI). The catalyst is thus rendered as an iron(III) hydroxide, which again is most stable in its high spin form with respect to the energetically closest spin state, in this case the quartet ($\Delta G^{\text{HF-DLPNO-CCSD(T)}}$ = 23.8 kcal mol^{-1}). Formation of the iron–OBpin species from the iron hydroxide is further downhill at $\Delta_r G$ = –61.3 kcal mol^{-1}. The overall reaction of this first half-cycle, i.e., the reduction of the nitro to the nitroso species **4**, is exergonic by $\Delta_r G$ = –59.6 kcal mol^{-1}.

In the second half-cycle, the initial barrier for hydride transfer from **1c** to the nitroso species is found at $\Delta G^{\ddagger}$ = 15.8 kcal mol^{-1}, translating to $t_{1/2} \approx 43$ ms. This is distinctly lower than that of the rate limiting step for the initial nitro reduction, which is clearly in agreement with the experimental observation that **4** does not appreciably build up in the reaction. The N-hydroxy intermediate lies at $\Delta_r G$ = –37.4 kcal mol^{-1}. Further reduction to the iron amido species is again strongly exergonic ($\Delta_r G$ = –108.3 kcal mol^{-1}). For the net reduction reaction of the nitroso intermediate to the product **2** in the second half cycle, the Gibbs energy amounts to $\Delta_r G$ = –117.4 kcal mol^{-1}.

For nitrobenzene, the same general picture emerges, though with a lower rate-limiting first reduction step of $\Delta G^{\ddagger}$ = 15.6 kcal mol^{-1} (see SI). This would correspond to an approximate acceleration in $t_{1/2}$ by three orders of magnitude, which is consistent with the experimental finding of a much more rapid reactivity for nitrobenzene than 2-nitropropane.

For completeness, we note that a lower-energy low spin form of the rate-limiting TS can be found with DFT, which suffers, however, from significant spin contamination. HF-DLPNO-CCSD(T1) calculations report a less stable low-spin than high spin state, albeit with a large T_1 diagnostic of 0.08 for the doublet (see Table S9). This arises from single excitations between almost degenerate molecular orbitals delocalized between iron and the NO moiety of the substrate (see Figure S335). Such a scenario was discussed recently for a singlet biradicaloid intermediate *en route* to Pd(II) nitrene reactivity.[54] Canonical HF-based coupled-cluster theory was found to suffer dramatic errors, whereas with more delocalized Kohn-Sham reference orbitals the CCSD(T) results improved substantially. We observe a similar trend for the low-spin TS, where KS reference orbitals lower the T_1 diagnostic to reasonable values below 0.04 (see Table S9). With KS-DLPNO-CCSD(T1), the low-spin TS is lower in energy than its HS congener.

Importantly though, regardless of spin state, the initial barrier for nitro reduction predicted with KS-DLPNO-CCSD(T1) agrees with the experimentally observed rate-determining step (see Table S8). It is therefore not possible to discriminate between the two spin state options by comparison with experiment. We emphasize that with both types of CC description, the TS of the first half-cycle is always higher in energy than that of the second half-cycle (see Figure S336). The only calculations where this would be predicted incorrectly are those using DFT, where the low-spin TS is suffering from artefacts due to spin contamination (see Figure S334, Table S8). If the route via the low-spin TS were the correct description, this would render the rate-determining step of the second half-cycle as the overall limiting step, in conflict with the experimental observations. We furthermore note that any purported intermediate-spin or low-spin transition structures would have to undergo a spin-orbit coupled spin-crossover twice between the corresponding reactant and product intermediate structures. An estimate of such spin-crossing probabilities is beyond the scope of this work. However, given the experimentally observed rapid reactivity and the high-spin description being consistent with the experimental information, we surmise that the high-spin surface will be more competitive during the catalytic cycle than a multistate scenario with several spin crossover impediments.

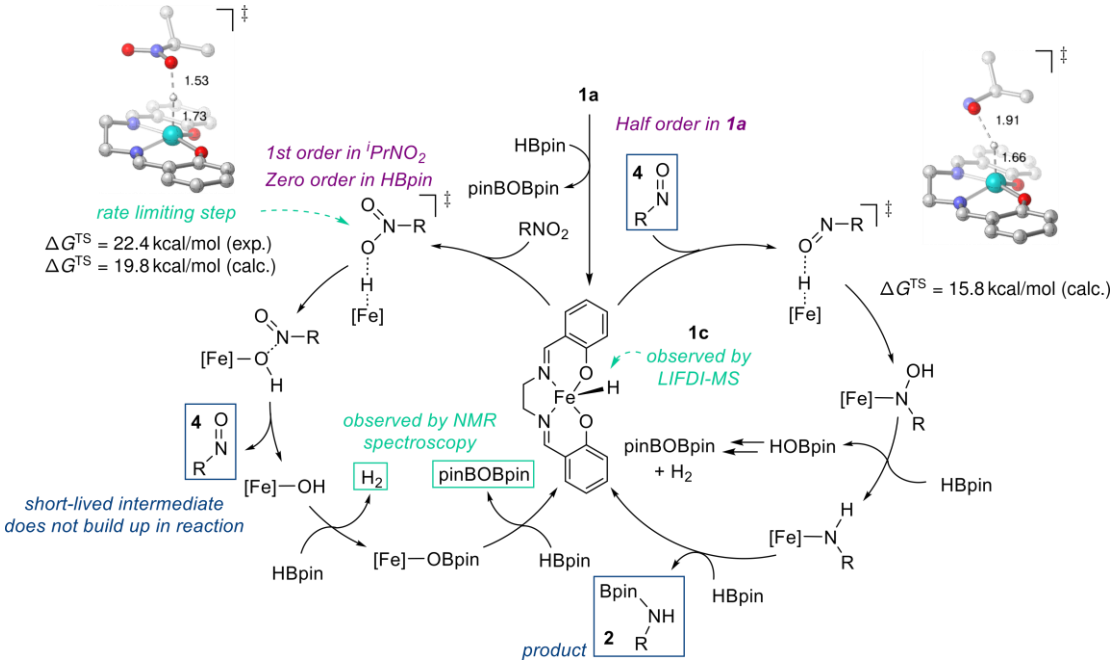

Figure 4. Postulated catalytic cycle proceeding via iron(III) hydride intermediate **1c**.

2.3 Hydroamination

Upon developing a greater understanding of the mechanism of nitro reduction, we believed that our catalytic system would be primed for an *in situ* HA of olefins, similar to that of Baran's study. Based on our identification of an iron-hydride as a potential intermediate in catalysis, and thereby comparison to observations made by Baran and co-workers, we hypothesized that our system would be competent in the *in situ* reductive functionalization of nitro compounds. This reaction does not operate via a standard HA protocol, where N–H adds across a C–C double or triple bond; the active iron hydride should facilitate the partial reduction of the nitro moiety (forming a nitroso intermediate)[55,56] and hydrogen atom transfer (HAT)[57] to the unsaturated coupling partner. The transformation relies on a nitroso intermediate reacting with an alkyl radical, followed by a series of reduction steps.[58]

We initiated our HA studies by reacting 4-*tert*-butylnitrobenzene with HBpin in the presence of allylbenzene and **1a** but found that only the aniline product (**2b**) was formed. From our initial reaction it was clear that HBpin is too active in the reduction process, therefore interception of a nitroso intermediate is not possible. However, use of H_3SiPh should slow the entire catalytic process down and thus facilitate HA. Reaction of **1a**, 4-*tert*-butylnitrobenzene, allylbenzene and H_3SiPh results in a small amount of HA product being observed by ^1H NMR spectroscopy. However, even after several rounds of optimization (see the Supporting Information) and screening two other substrates with differing electronic properties, HA is not able to outcompete reduction (to form 4-*tert*-butylaniline) or the double addition product formation (**9**), Table 1. Although not atom economic, these double functionalization products (of the form **9**) can be reduced using Zn/HCl in hot MeOH to cleave the N–O bond and generate the HA product, *e.g.* **8** from **9**. It quickly became apparent that a traditional screening approach would not be an efficient way to improve this catalysis and we hypothesized that the issue was more fundamental, namely that there was a mismatch between the SOMO of the iron hydride **1c** and the LUMO of the alkene being employed. Using density functional theory (PBEo-D3/def2-TZVP//PBE-D3/def2-SVP including an implicit solvation model for acetonitrile), we calculated the energy of the alkene LUMO (see Table 1). This clearly shows a range of energies, from very positive (1-methylcyclohexene, 0.54 eV) which gives the aniline almost exclusively, through to very negative (α-methylstyrene, –2.17 eV) which gives the double functionalization product (**9**) almost exclusively. At an intermediate energy (allyl benzene) we form a mixture of HA product (**8**) and aniline.

Table 1. Attempts at HA optimization demonstrate product distribution is linked to alkene LUMO energy.

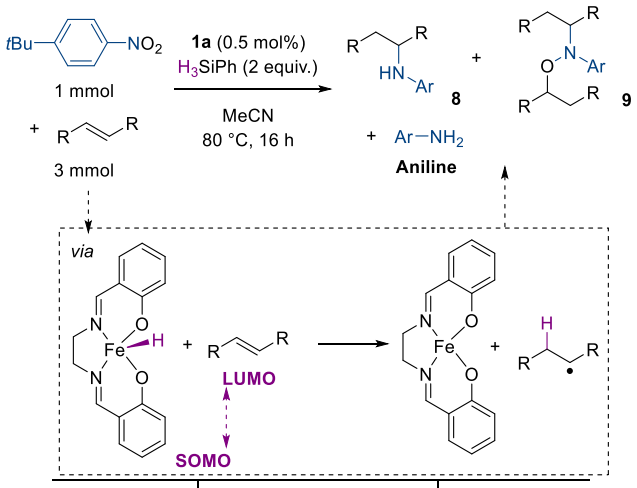

Alkene	Ratio of products			LUMO
	8	9	Aniline	Energy (eV)

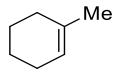	1	0	10	+0.54
	0.9	0	1	–0.50
	0.01	10.7	1	–1.16

We therefore wondered if we could use the LUMO energy from a DFT calculation of a given alkene as a simple predictive tool for its competency in HA. We selected a range of alkenes with LUMO energies that span from -2.17 eV (ethyl cinnamate) up to 1-methylcyclohexene at +0.54 eV and applied these in HA using the conditions optimized for allylbenzene. The energy of the SOMO of **1c** is calculated to be –6.08 eV (see the Supporting Information). Gratifyingly, a general trend is observed (Chart 1, isolated yields shown in Table 2) whereby alkenes with very positive LUMO energies tend not to react and over-reduction to form 4-*tert*-butylaniline dominates (clearly the SOMO/LUMO gap is too large in this case). In contrast, as we move to more negative LUMO energies the HA reaction (generating **8** and/or **9**) begins to dominate. However, for ethyl cinnamate no product is observed and an insoluble precipitate forms; this is likely due to polymerization of the alkene as the more stable radical builds up in the system. Therefore, we can conclude that simple LUMO calculations can be used as a qualitative guide to predict reactivity of an alkene. For instance, an alkene with a LUMO energy of 0.00 eV is likely to give only a modest (approximately 15%) amount of **8** and **9**, whereas an alkene with a LUMO energy of –0.95 eV is likely to give approximately 85% of products **8** and **9**. The ability to predict **8** versus **9** is not possible using this simple qualitative measure, but some general trends can be established (see the Supporting Information for a chart showing the LUMO energy versus the yields of **8**, **9** and aniline data presented in Table 2, entries 1 to 10).

Chart 1. The ability of 1a to undertake HA catalysis is inherently linked to the LUMO energy of the alkene coupling partner.

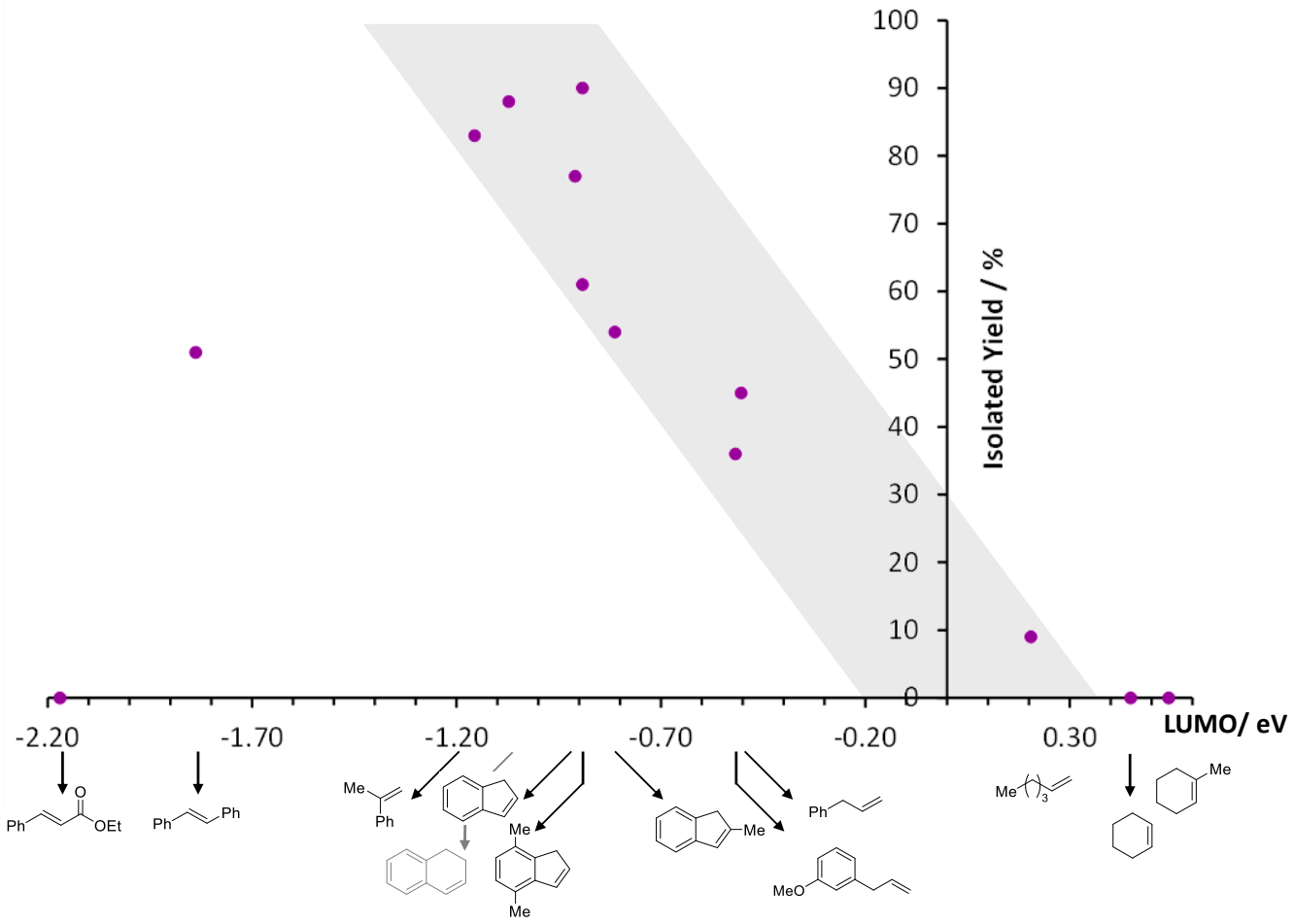

Clearly the optimum substrates to use for HA have a LUMO energy of approximately –1 eV (indenes, 1,2-dihydronaphthalene and styrenes). In contrast, non-activated alkenes are not suitable for catalysis (allyl benzenes through

to cyclic and acyclic aliphatic alkenes). This provides a nice level of complementarity to the work of Baran, where HA failed with styrenes, but outcompetes our catalyst's ability to undertake HA on aliphatic substrates. Based on our studies to-date, this is likely due to the difference in the electronic nature of the two different iron-hydrides being formed (from **1a** versus $Fe(acac)_3$[27] as the pre-catalysts).

In order to prove the hypothesis that alkenes with LUMO energies of approximately –1 eV will perform well and those with LUMO energies ≥ –0.5 eV will perform poorly, we undertook a more detailed substrate scope study (Table 2).[59] We have further expanded the scope to investigate 4-fluoroallylbenzene (Entry 11), which shows no discernable sign of the *N*,*O*-alkylated product (**9k**) and **8k** is isolated in 50% yield. Benzo[*b*]thiophene does not behave like benzofuran with the former only giving 19% **8l** (Entry 12) and 65% 4-*tert*-butylaniline compared to 61/35% of **8f**/**9f** for benzofuran (Entry 6). Boc-protected indole does allow HA with the protecting group remaining intact, but only 20% **8m** and 70% spectroscopic yield of the aniline is obtained (Entry 13). As expected, changing to nitrobenzene gives similar HA results as 4-*tert*-buylnitrobenzene (compare entries 2, 4, 8 and 9 to entries 14 to 17). Changing the electronics of the nitro aromatic compound has some effect on the ratio of products formed, but overall, the isolated yield of the HA product is good. For example methyl(4-nitrophenyl)sulfane reacts with indene to give **8t** in 63% isolated yield (Entry 20), 1-nitro-4-(trifluoromethyl)benzene reacts with indene to give **8w** in 23% isolated yield, **9w** in 54%, and a combined yield following Zn/HCl reduction of 60% (Entry 23). Pleasingly, even sterically challenging nitro aromatics, such as 2-methyl-1-nitronaphthalene can be applied under our general HA conditions, generating the indenyl product **8y** in 16% isolated yield and the *N*,*O*-alkylated species, **9y**, in 45% (Entry 25). As expected, across all nitro aromatics, 3-methoxyallylbenzene does not perform well (Entries 8, 16 and 21). It is worth noting that isolated yields are reported, with spectroscopic yields being challenging due to the complex nature of the ^{1}H NMR spectra of the crude reaction mixtures.

Table 2. Probing the substrate dependency on the LUMO energy for the HA of nitroarenes.

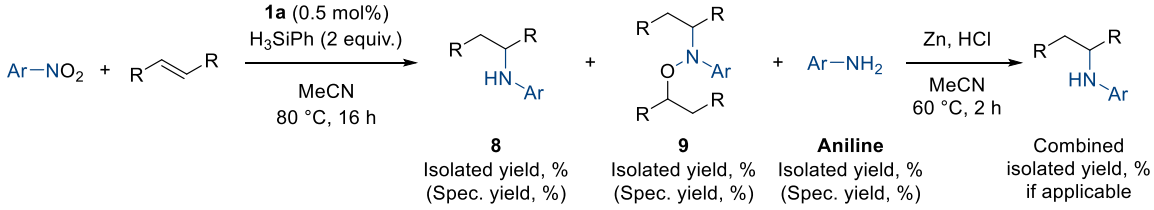

	Nitroarene	Alkene	HA product		8	9	Aniline	Combined yield
1	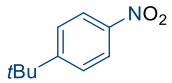	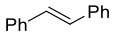	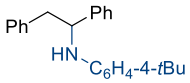	8a	37	14	44	-
2			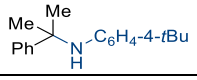	8b	0	83	-	32
3		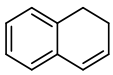	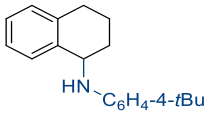	8c	24	64	-	75
4		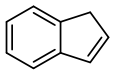	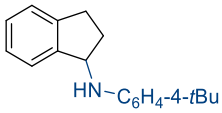	8d	77	0	-	-
5		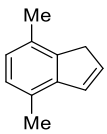	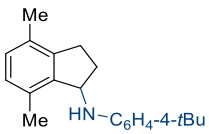	8e	18	72	-	71
6		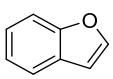	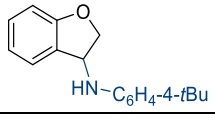	8f	61	-	(35)	-
7		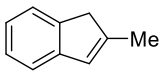	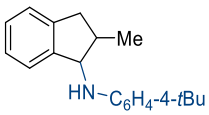	8g	-	-	(40)	54

8		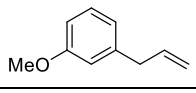	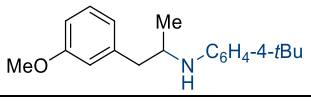	8h	36	(0)	(33)	-
9		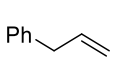	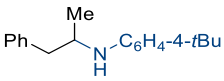	8i	45	(0)	(47)	-
10		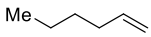	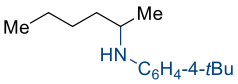	8j	5	(4)	87	-
11		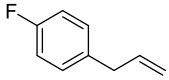	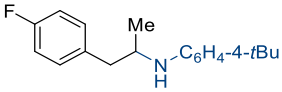	8k	50	(0)	50	-
12		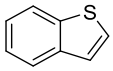	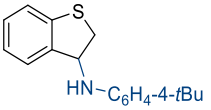	8l	19	(0)	65	-
13		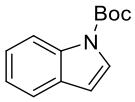	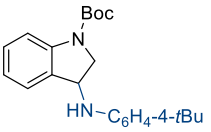	8m	20	(0)	(70)	-
14	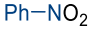		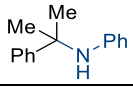	8n	0	89	-	-
15		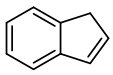	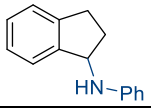	8o	31	67	-	77
16[a]		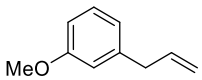	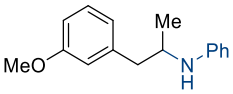	8p	31	(0)	-	-
17[a]			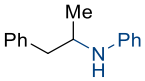	8q	36	(0)	-	-
18	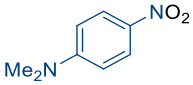	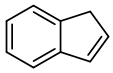	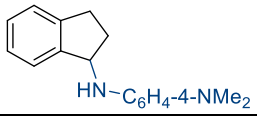	8r	33 (60)	(0)	-	-
19	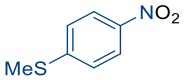		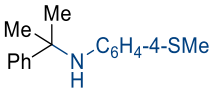	8s	24	71	-	-
20		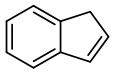	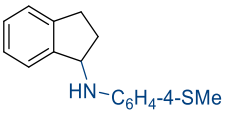	8t	63	(0)	-	-
21[a]		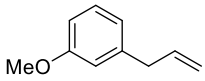	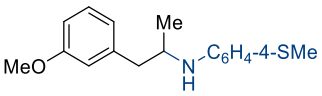	8u	37	(0)	-	-
22[a]		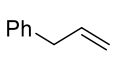	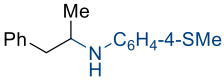	8v	43	(0)	-	-
23	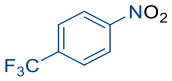	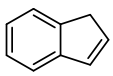	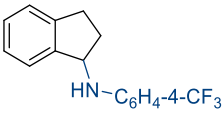	8w	23	54	-	60
24		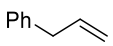	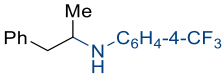	8x	22	16	47	-

25	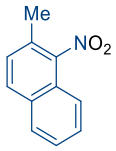	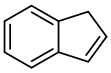	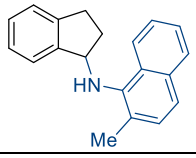	8y	16	45	-	-

Conditions: 1 mmol nitro compound, 3 mmol alkene, 0.5 mol% **1a**, 2 mmol H_3SiPh, 0.5 mL MeCN, 80 °C, 16 h. Isolated yields reported. Spectroscopic yield is provided in parentheses. All spectroscopic yields are based on UHPLC data calibrated against an internal standard. If yield is not reported, the mass balance was deemed sufficient without this additional data point. [a]Remainder of the yield was primary amine, identified by UPLC, but not isolated.

Similar to the nitro reduction, EPR studies in the presence of **1a** and spin trapping agent DMPO (5,5-dimethyl-1-pyrroline-*N*-oxide) generate the hydrogen-atom trapping product DMPO-H. Unfortunately, no alkyl radicals are detected under catalytic conditions (recorded at 298 K) in the presence of *trans*-stilbene, indene or 1-hexene (Figure 5). When PBN (phenyl *N*-*tert*-butylnitrone) is employed, there is also some evidence for silane- and amine-adducts of PBN being formed at 298 K, but once again there is no direct evidence for the presence of alkyl radicals (see the Supporting Information). We are pleased to be able to report strong evidence for HAT through these EPR studies, even though no alkyl radicals are detected; we expect these to be short-lived intermediates so their detection is not trivial.

Further control reactions also support a cycle that involves alkyl radical generation and trapping by a nitroso intermediate. For example, reaction of **1a**, 4-*tert*-butylaniline, allylbenzene and H_3SiPh does not give secondary amine product, but the anti-Markovnikov hydrosilylation product, phenyl(3-phenylpropyl)silane, forms in trace amounts (7%) along with trace propyl benzene (4%). The anti-Markovnikov hydrosilylation product forms quantitatively when 1-hexene is employed in the reaction of reaction of **1a**, 4-*tert*-butylaniline and H_3SiPh. These are clearly not the product of a radical reaction and the presence of a nitro/nitroso species is necessary for HA, doing so in a Markovnikov fashion *i.e. via* the most stable alkyl radical.

Reaction of **1a** (0.5 mol%), nitrosobenzene (1 mmol), indene (3 mmol) and H_3SiPh (2 mmol) gives 38% azobenzene (**6a'**), 10% (**80**) and trace aniline, indicating the nitroso is active in catalysis but must not build up to any extent under our standard HA conditions. In other words, in high concentrations, the nitroso is sequestered in competing side-reactions. Reaction of indene (3 mmol), H_3SiPh (2 mmol) and **1a** (0.5 mol%) gives oligomeric material, as evidenced by DOSY NMR spectroscopy (see the Supporting Information). In the absence of a suitable trapping reagent (nitroso compound) radical polymerization dominates. This, coupled with the observation that allylbenzene generates propyl benzene (*vide infra*) albeit in small quantities, indicates that the transformation could be occurring via HAT.

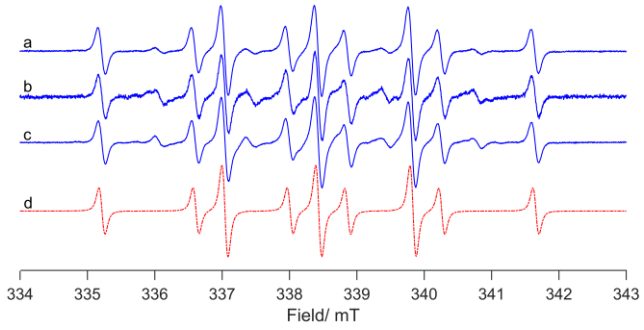

Figure 5. CW EPR spectra (T = 298 K) of the reaction of **1a** with $PhSiH_3$, $C_6H_5NO_2$ and (a) *trans*-stilbene, (b) indene, and (c) hexene in the presence of DMPO. The simulation of a trapped H-DMPO adduct is given in (d).

CONCLUSION

In summary, we have applied the simple catalytic pairing of **1a** and HBpin to enable the facile reduction of nitro organics. We have used reaction tuning through the choice of reductant to give chemoselectivity in the presence of other reducible functional groups. The mechanism was studied using a range of analytical techniques such as EPR and LIFDI-MS and –coupled with kinetic studies and electronic structure investigations on postulated key intermediates– we can propose a reaction mechanism that proceeds via two catalytic cycles interlinked via a key iron hydride complex. HBpin is too active to allow access to a hydroamination catalytic cycle, but once again, using a less active reductant does allow for effective HA. We have shown that a simple MO-based predictor from DFT calculations can be used to assess the suitability of an alkene for use in HA reactions. With the high levels of electronic tuning available to us through salen ligand modification, we should be able to tune the SOMO energy of the pre-catalyst and thus modify our ability to undertake HA of different alkenes; this is an interesting hypothesis and one that we are currently testing.

ASSOCIATED CONTENT

Supporting Information

Analysis data and NMR spectra for all products is provided in the supporting information (PDF file). Computational supporting information is also provided which contains all data relevant to the computational studies reported here, including methodology, benchmarking studies, energetics and coordinates of characterized stationary pointsThe Supporting Information is available free of charge on the ACS Publications website.

AUTHOR INFORMATION

Corresponding Author

* Dr. Emma Richards, richardse10@cardiff.ac.uk

* Prof. Vera Krewald, vera.krewald@tu-darmstadt.de

* Dr. Ruth L. Webster, rw740@cam.ac.uk

Author Contributions

Manuscript prepared through contributions from all authors.

Notes

The authors declare no competing financial interests.

ACKNOWLEDGMENT

The EPSRC (RLW), Leverhulme Trust (RLW, TMH, MD, VK) and Astra Zeneca (EP) are thanked for funding. Cei Provis-Evans is thanked for initial studies into the reduction of nitromethane, 1-methoxy-3-nitrobenzene, 2-nitropropane and 1-nitropentane. Calculations for this research were conducted on the Lichtenberg high performance computer of the TU Darmstadt. We would like to thank Professor Ian Fairlamb and Karl Heaton (University of York) for instrument time and assistance with LIFDI-MS measurements. We also appreciate assistance from Dr. John Lowe and Dr. Kathryn Proctor (Core Research Facility, University of Bath) for assistance with DOSY NMR and MS analysis, respectively. Professor Simon Lewis is acknowledged for lab-based support (EP).

REFERENCES

(1) Oxidations and Reductions. In *March's Advanced Organic Chemistry*, 2006; pp 1703-1869.

(2) Ueber die Einwirkung der Eisenoxydulsalze auf Nitronaphtalin und Nitrobenzol. *Justus Liebigs Ann. Chem.***1854**, *92* (3), 401-403.

(3) Agrawal, A.; Tratnyek, P. G. Reduction of Nitro Aromatic Compounds by Zero-Valent Iron Metal. *Environ. Sci. Technol.* **1996**, *30* (1), 153-160.

(4) Orlandi, M.; Brenna, D.; Harms, R.; Jost, S.; Benaglia, M. Recent Developments in the Reduction of Aromatic and Aliphatic Nitro Compounds to Amines. *Org. Process Res. Dev.* **2018**, *22* (4), 430-445.

(5) Wu, J.; Darcel, C. Recent Developments in Manganese, Iron and Cobalt Homogeneous Catalyzed Synthesis of Primary Amines via Reduction of Nitroarenes, Nitriles and Carboxamides. *Adv. Synth. Catal.* **2023**, *365* (7), 948-964.

(6) Rana, S.; Biswas, J. P.; Paul, S.; Paik, A.; Maiti, D. Organic synthesis with the most abundant transition metal–iron: from rust to multitasking catalysts. *Chem. Soc. Rev.* **2021**, *50* (1), 243-472.

(7) Sunada, Y.; Kawakami, H.; Imaoka, T.; Motoyama, Y.; Nagashima, H. Hydrosilane Reduction of Tertiary Carboxamides by Iron Carbonyl Catalysts. *Angew. Chem. Int. Ed.* **2009**, *48* (50), 9511-9514.

(8) Junge, K.; Wendt, B.; Shaikh, N.; Beller, M. Iron-catalyzed selective reduction of nitroarenes to anilines using organosilanes. *Chem. Commun.* **2010**, *46* (10), 1769-1771.

(9) Pehlivan, L.; Métay, E.; Laval, S.; Dayoub, W.; Demonchaux, P.; Mignani, G.; Lemaire, M. Iron-catalyzed selective reduction of nitro compounds to amines. *Tetrahedron Lett.* **2010**, *51* (15), 1939-1941.

(10) Pehlivan, L.; Métay, E.; Laval, S.; Dayoub, W.; Demonchaux, P.; Mignani, G.; Lemaire, M. Alternative method for the reduction of aromatic nitro to amine using TMDS-iron catalyst system. *Tetrahedron* **2011**, *67* (10), 1971-1976.

(11) Zhu, K.; Shaver, M. P.; Thomas, S. P. Chemoselective nitro reduction and hydroamination using a single iron catalyst. *Chem. Sci.* **2016**, *7* (5), 3031-3035.

(12) Wu, J.; Tongdee, S.; Ammaiyappan, Y.; Darcel, C. A Concise Route to Cyclic Amines from Nitroarenes and Ketoacids under Iron-Catalyzed Hydrosilylation Conditions. *Adv. Synth. Catal.* **2021**, *363* (15), 3859-3865.

(13) Shaikh, N. S. Sustainable Amine Synthesis: Iron Catalyzed Reactions of Hydrosilanes with Imines, Amides, Nitroarenes and Nitriles. *ChemistrySelect* **2019**, *4* (22), 6753-6777.

(14) Verma, P. K.; Bala, M.; Thakur, K.; Sharma, U.; Kumar, N.; Singh, B. Iron and Palladium(II) Phthalocyanines as Recyclable Catalysts for Reduction of Nitroarenes. *Catal. Lett.* **2014**, *144* (7), 1258-1267.

(15) Gao, Y.; Yang, S.; Huo, Y.; Hu, X.-Q. Recent Progress on Reductive Coupling of Nitroarenes by Using Organosilanes as Convenient Reductants. *Adv. Synth. Catal.* **2020**, *362* (19), 3971-3986.

(16) Kadam, H. K.; Tilve, S. G. Advancement in methodologies for reduction of nitroarenes. *RSC Adv.* **2015**, *5* (101), 83391-83407.

(17) Murata, S.; Miura, M.; Nomura, M. Reduction of aromatic nitro compounds with 2-mercaptoethanol and oxidation of thiophenol with molecular oxygen mediated by trinuclear iron acetate complexes. *J. Chem. Soc. Perkin Trans.* **1989**, (6), 617-621.

(18) Sharma, U.; Verma, P. K.; Kumar, N.; Kumar, V.; Bala, M.; Singh, B. Phosphane-Free Green Protocol for Selective Nitro Reduction with an Iron-Based Catalyst. *Chem. Eur. J.* **2011**, *17* (21), 5903-5907.

(19) MacNair, A. J.; Tran, M.-M.; Nelson, J. E.; Sloan, G. U.; Ironmonger, A.; Thomas, S. P. Iron-catalysed, general and operationally simple formal hydrogenation using Fe(OTf)3 and NaBH4. *Org. Biomol. Chem.* **2014**, *12* (28), 5082-5088.

(20) Cantillo, D.; Baghbanzadeh, M.; Kappe, C. O. In Situ Generated Iron Oxide Nanocrystals as Efficient and Selective Catalysts for the Reduction of Nitroarenes using a Continuous Flow Method. *Angew. Chem. Int. Ed.* **2012**, *51* (40), 10190-10193.

(21) Wilkinson, H. S.; Tanoury, G. J.; Wald, S. A.; Senanayake, C. H. Chemoselective reductions of nitroarenes: bromoethanol-assisted phthalocyanatoiron/NaBH4 reductions. *Tetrahedron Lett.* **2001**, *42* (2), 167-170.

(22) Deshpande, R. M.; Mahajan, A. N.; Diwakar, M. M.; Ozarde, P. S.; Chaudhari, R. V. Chemoselective Hydrogenation of Substituted Nitroaromatics Using Novel Water-Soluble Iron Complex Catalysts. *J. Org. Chem.* **2004**, *69* (14), 4835-4838.

(23) Wienhöfer, G.; Sorribes, I.; Boddien, A.; Westerhaus, F.; Junge, K.; Junge, H.; Llusar, R.; Beller, M. General and Selective Iron-Catalyzed Transfer Hydrogenation of Nitroarenes without Base. *J. Am. Chem. Soc.* **2011**, *133* (32), 12875-12879.

(24) Wienhöfer, G.; Baseda-Krüger, M.; Ziebart, C.; Westerhaus, F. A.; Baumann, W.; Jackstell, R.; Junge, K.; Beller, M. Hydrogenation of nitroarenes using defined iron–phosphine catalysts. *Chem. Commun.* **2013**, *49* (80), 9089-9091.

(25) Jagadeesh, R. V.; Wienhöfer, G.; Westerhaus, F. A.; Surkus, A.-E.; Pohl, M.-M.; Junge, H.; Junge, K.; Beller, M. Efficient and highly selective iron-catalyzed reduction of nitroarenes. *Chem. Commun.* **2011**, *47* (39), 10972-10974.

(26) Chen, X.; Wang, H.; Du, S.; Driess, M.; Mo, Z. Deoxygenation of Nitrous Oxide and Nitro Compounds Using Bis(N-Heterocyclic Silylene)Amido Iron Complexes as Catalysts. *Angew. Chem. Int. Ed.* **2022**, *61* (7), e202114598.

(27) Gui, J.; Pan, C.-M.; Jin, Y.; Qin, T.; Lo, J. C.; Lee, B. J.; Spergel, S. H.; Mertzman, M. E.; Pitts, W. J.; La Cruz, T. E.; Schmidt, M. A.; Darvatkar, N.; Natarajan, S. R.; Baran, P. S. Practical olefin hydroamination with nitroarenes. *Science* **2015**, *348* (6237), 886-891.

(28)Song, H.; Yang, Z.; Tung, C.-H.; Wang, W. Iron-Catalyzed Reductive Coupling of Nitroarenes with Olefins: Intermediate of Iron–Nitroso Complex. *ACS Catal.* **2020**, *10* (1), 276-281.

(29) Zou, D.; Wang, W.; Hu, Y.; Jia, T. Nitroarenes and nitroalkenes as potential amino sources for the synthesis of N-heterocycles. *Org. Biomol. Chem.* **2023**, *21* (11), 2254-2271.

(30) Driver, T. G. Unlocking Electrophilic N-Aryl Intermediates from Aryl Azides, Nitroarenes, and Aryl Amines in Cyclization–Migration Reactions. *Synlett* **2022**, *33* (19), 1890-1901.

(31) Crotti, C.; Cenini, S.; Rindone, B.; Tollari, S.; Demartin, F. Deoxygenation reactions of ortho-nitrostyrenes with carbon monoxide catalysed by metal carbonyls: a new route to indoles. *J. Chem. Soc. Chem. Commun.* **1986**, (10), 784-786.
(32) Shevlin, M.; Guan, X.; Driver, T. G. Iron-Catalyzed Reductive Cyclization of o-Nitrostyrenes Using Phenylsilane as the Terminal Reductant. *ACS Catal.* **2017**, *7* (8), 5518-5522.
(33) Vu, V.; Powell, J. N.; Ford, R. L.; Patel, P. J.; Driver, T. G. Development and Mechanistic Study of an Iron-Catalyzed Intramolecular Nitroso Ene Reaction of Nitroarenes. *ACS Catal.* **2023**, *13* (22), 15175-15181.
(34) Waheed, M.; Alsharif, M. A.; Alahmdi, M. I.; Mukhtar, S.; Parveen, H. Iron-catalyzed intramolecular reductive cyclization of o-nitroarenes to indoles under visible light irradiation. *Tetrahedron Lett.* **2023**, *123*, 154543.
(35) Tran, C.; Abdallah, A.; Duchemann, V.; Lefèvre, G.; Hamze, A. Iron-catalyzed reductive cyclization of nitroarenes: Synthesis of aza-heterocycles and DFT calculations. *Chin. J. Chem.***2023**, *34* (3), 107758.
(36) Gallagher, K. J.; Webster, R. L. Room temperature hydrophosphination using a simple iron salen pre-catalyst. *Chem. Commun.* **2014**, *50* (81), 12109-12111.
(38) Gallagher, K. J.; Espinal-Viguri, M.; Mahon, M. F.; Webster, R. L. A Study of Two Highly Active, Air-Stable Iron(III)-μ-Oxo Precatalysts: Synthetic Scope of Hydrophosphination using Phenyl- and Diphenylphosphine. *Adv. Synth. Catal.* **2016**, *358* (15), 2460-2468.
(39) Lau, S.; Provis-Evans, C. B.; James, A. P.; Webster, R. L. Hydroboration of aldehydes, ketones and CO_2 under mild conditions mediated by iron(III) salen complexes. *Dalton Trans.* **2021**, *50* (31), 10696-10700.
(40) Provis-Evans, C. B.; Lau, S.; Krewald, V.; Webster, R. L. Regioselective Alkyne Cyclotrimerization with an In Situ-Generated [Fe(II)H(salen)]·Bpin Catalyst. *ACS Catal.* **2020**, *10* (17), 10157-10168.
(41) Hood, T. M.; Lau, S.; Diefenbach, M.; Firmstone, L.; Mahon, M.; Krewald, V.; Webster, R. L. The Complex Reactivity of [(salen)Fe]2(μ-O) with HBpin and Its Implications in Catalysis. *ACS Catal.* **2023**, *13* (17), 11841-11850.
(42) Canali, L.; C. Sherrington, D. Utilisation of homogeneous and supported chiral metal(salen) complexes in asymmetric catalysis. *Chem. Soc. Rev.* **1999**, *28* (2), 85-93.
(43) Cozzi, P. G. Metal–Salen Schiff base complexes in catalysis: practical aspects. *Chem. Soc. Rev.* **2004**, *33* (7), 410-421.
(44) Kleij, A. W. Nonsymmetrical Salen Ligands and Their Complexes: Synthesis and Applications. *Eur. J. Inorg. Chem.* **2009**, *2009* (2), 193-205.
(45) Whiteoak, C. J.; Salassa, G.; Kleij, A. W. Recent advances with π-conjugated salen systems. *Chem. Soc. Rev.* **2012**, *41* (2), 622-631.
(46) Shaw, S.; White, J. D. Asymmetric Catalysis Using Chiral Salen–Metal Complexes: Recent Advances. *Chem. Rev.* **2019**, *119* (16), 9381-9426.
(47) Fochi, G.; Floriani, C. The role of titanium and iron complexes in the deoxygenation of aromatic nitroso-compounds. *J. Chem. Soc. Dalton Trans.* **1984**, (11), 2577-2580.
(48) Earnshaw, A.; King, E. A.; Larkworthy, L. F. Transition metal–Schiff's base complexes. Part V. Spin equilibria in some iron mononitrosyls. *J. Chem. Soc. A.* **1969**, (0), 2459-2463.
(49) Adding TEMPO (1 equiv. relative to nitro) to 4-*N*,*N*-dimethylnitrobenzene gives 59% product **3c** and 13% free aniline after 20 min at RT when TEMPO is added to the reaction mixture last. When TEMPO is added before HBpin 64% **3c** and 3% free aniline is obtained relative to an internal standard. In short, the nitro reduction is not shut down and we therefore feel radicals are not involved in catalysis.
(50) Burés, J. Variable Time Normalization Analysis: General Graphical Elucidation of Reaction Orders from Concentration Profiles. *Angew. Chem. Int. Ed.* **2016**, *55* (52), 16084-16087.
(51) Hawthorne, M. F.; Lewis, E. S. Amine Boranes. III. Hydrolysis of Pyridine Diphenylborane and the Mechanism of Hydride Transfer Reactions. *J. Am. Chem. Soc.* **1958**, *80* (16), 4296-4299.
(52) Kaplan, L.; Wilzbach, K. E. Hydrogen Isotope Effects in the Alkaline Cleavage of Triorganosilanes1. *J. Am. Chem. Soc.* **1955**, *77* (5), 1297-1302.
(53) Wiberg, K. B. The Deuterium Isotope Effect of Some Ionic Reactions of Benzaldehyde. *J. Am. Chem. Soc.* **1954**, *76* (21), 5371-5375.
(54) Verplancke, H.; Diefenbach, M.; Lienert, J. N.; Ugandi, M.; Kitsaras, M.-P.; Roemelt, M.; Stopkowicz, S.; Holthausen, M. C. Another Torture Track for Quantum Chemistry: Reinvestigation of the Benzaldehyde Amidation by Nitrogen-Atom Transfer from Platinum(II) and Palladium(II) Metallonitrenes. *Isr. J. Chem.* **2023**, *63* (7-8), e202300060.
(55) Brown, H. C.; Azzaro, M. E.; Koelling, J. G.; McDonald, G. J. Secondary Isotope Effects in the Reactions of Methyl-d3-pyridines with Boron Trifluoride. Consideration of the Secondary Isotope Effect as a Steric Phenomenon1,2. *J. Am. Chem. Soc.* **1966**, *88* (11), 2520-2525.
(56) That a nitroso forms efficiently and is trapped out during the reaction is key, otherwise there could be a competing hydration process, similar to that reported by Studer: Bhunia, A.; Bergander, K.; Daniliuc, C. G.; Studer, A. Fe-Catalyzed Anaerobic Mukaiyama-Type Hydration of Alkenes using Nitroarenes. *Angew. Chem. Int. Ed.* **2021**, *60*, 8313-8320.
(57) Shevick, S. L.; Wilson, C. V.; Kotesova, S.; Kim, D.; Holland, P. L.; Shenvi, R. A. Catalytic hydrogen atom transfer to alkenes: a roadmap for metal hydrides and radicals. *Chem. Sci.* **2020**, 11 (46), 12401-12422.
(58) See the Supporting Information of Reference 27.
(59) In the case of Entry 2 (Table 2), we note that α-methyl styrene is challenging to reduce using Zn/HCl, hence the reduced isolated yield from this reaction. Attempts at an alternative reduction using Raney Ni and H_2 also failed.